

VisualGPT: Data-efficient Adaptation of Pretrained Language Models for Image Captioning

Jun Chen¹, Han Guo², Kai Yi¹, Boyang Li³, Mohamed Elhoseiny¹

¹ King Abdullah University of Science and Technology (KAUST),

²Carnegie Mellon University, ³ Nanyang Technological University

{jun.chen, kai.yi, mohamed.elhoseiny}@kaust.edu.sa

hanguo@cs.cmu.edu, boyang.li@ntu.edu.sg

Abstract

The limited availability of annotated data often hinders real-world applications of machine learning. To efficiently learn from small quantities of multimodal data, we leverage the linguistic knowledge from a large pre-trained language model (PLM) and quickly adapt it to new domains of image captioning. To effectively utilize a pretrained model, it is critical to balance the visual input and prior linguistic knowledge from pretraining. We propose VisualGPT, which employs a novel self-resurrecting encoder-decoder attention mechanism to quickly adapt the PLM with a small amount of in-domain image-text data. The proposed self-resurrecting activation unit produces sparse activations that prevent accidental overwriting of linguistic knowledge. When trained on 0.1%, 0.5% and 1% of the respective training sets, VisualGPT surpasses the best baseline by up to 10.0% CIDEr on MS COCO [43] and 17.9% CIDEr on Conceptual Captions [63]. Furthermore, VisualGPT achieves the state-of-the-art result on IU X-ray [15], a medical report generation dataset. Our code is available at <https://github.com/Vision-CAIR/VisualGPT>.

1. Introduction

Recent performance gains in image captioning [13, 24, 28, 31, 75] are achieved on top of large-scale data corpora such as MS COCO [43] or Conceptual Captions [63], each containing hundreds of thousands of captions. Manual annotation of captions requires considerable time and effort. On the other hand, semi-automatic collection of image-caption pairs from the Internet, as used by Conceptual Captions [63], may generate incorrect or undesirable training data even after multiple rounds of cleaning. Data for specialized domains like medical report generation [15, 40] and low-resource language captioning [18, 74] cannot be easily

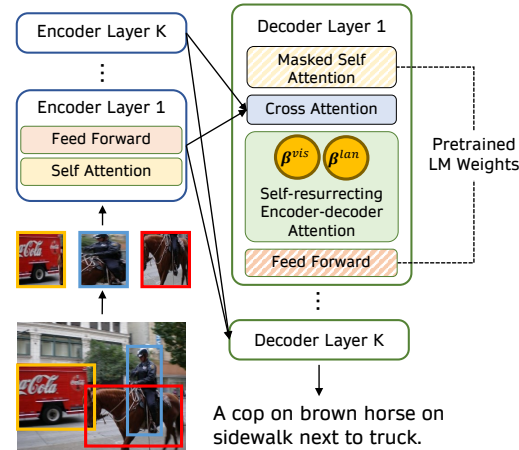


Figure 1. Our VisualGPT model transfers the knowledge from a pre-trained language model to the caption decoder. A self-resurrecting encoder-decoder attention is designed to connect the multi-level visual features and caption decoder.

scaled. Improving the data efficiency of image captioning networks would enable quick data curation, description of rare objects, and applications in specialized domains.

In this paper, we investigate the data efficiency problem for image captioning. This problem is distinct from the novel object captioning problem [1, 23], which relies on abundant in-domain data but zero out-of-domain data. Instead, we aim to improve the performance of image captioning systems trained on a small subset of *in-domain* data.

We propose to improve data efficiency by leveraging pre-trained language models (PLMs) [17, 34, 46, 60], such as BERT [16], XLNet [77], and GPT [6, 58, 59]. Via self-supervised learning, these models acquire rich linguistic and semantic knowledge, which has been shown to inform downstream tasks in NLP [7, 21]. However, the adaptation of PLMs pretrained on unimodal textual data for multimodal tasks remain under-investigated.

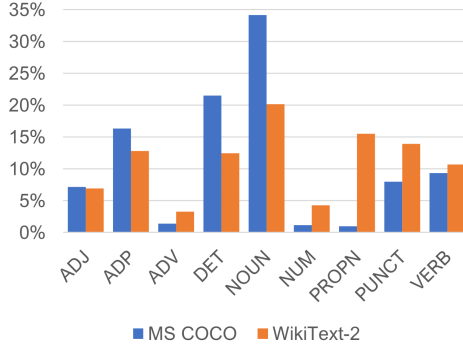


Figure 2. Comparison of the part-of-speech distributions of the MS COCO and WikiText-2 datasets [51]. We use the spacy parser and show only the most important categories.

A key challenge in utilizing PLMs is to bridge the domain gap between multi-modal data and the unimodal textual data the PLMs are pre-trained on. In Figure 2, we compare the part-of-speech distributions of MS COCO and WikiText-2 [51]. MS COCO employs 75% more nouns but 14% fewer verbs, which indicates a bias toward descriptions of static objects rather than actions. This suggests that, in order to effectively utilize PLMs in image captioning, we must balance prior linguistic knowledge acquired from pre-training and visual input information.

Figure 1 depicts the overall architecture of our proposed model, dubbed as VisualGPT. In the commonly used encoder-decoder architecture for image captioning, we initialize the parameters of the decoder from PLMs such as GPT-2 [59], whereas the encoder layers are randomly initialized. In addition, we propose an attention mechanism with self-resurrecting activation units (SRAUs), which balances the input from the visual encoder and the linguistic input from the previous decoder layer. The proposed mechanism can produce sparse activations while not being as vulnerable to the zero-gradient problem as regular gates; the self-resurrecting gates can be “turned on” again after being zeroed out.

Empirical results demonstrate that, when trained on 0.1%, 0.5%, and 1% of the MS COCO and Conceptual Captions data, VisualGPT outperforms several strong baseline models. We achieve the state-of-the-art result on IU X-ray [15], a medical report generation dataset. With several ablation experiments, we verify the effectiveness of PLMs and the proposed self-resurrecting attention mechanism.

Contributions. We make the following contributions:

- We explore the data efficiency problem for image captioning by utilizing pretrained language models (PLMs) as the caption decoder. With only a small amount of in-domain training data, the proposed technique quickly adapts PLMs to the cross-modal task of

image captioning. To our knowledge, this is the first work that focuses on efficiently adapting large pretrained language models for image captioning.

- We propose a novel encoder-decoder attention with self-resurrecting activation units (SRAUs), which can balance features from the visual and textual modalities. SRAU produces sparse activations that reduce accidental overwriting of pretrained weights.

2. Related Work

Image Captioning. Image captioning has been extensively studied in computer vision research. Early methods [19, 31, 37, 65, 79] focus on filling templates with extracted objects, attributes, and relationships. With the advent of deep learning, researchers proposed end-to-end neural networks that encode an image into vector representations and decode a caption word by word [27, 71]. Many improvements to the encoder [11, 38, 49, 75, 76, 80, 81], the decoder [72, 73, 78], and the attention mechanism [8, 13, 24, 33, 36] has since been proposed. Encoding the image using object regions has proven beneficial [2]. Reinforcement learning enables model optimization with non-differentiable evaluation metrics [14, 45, 61, 64]. [9, 12] investigate fine-grained control of caption generation. [14, 64] adopt GAN-like architectures that encourage human-like captions.

A few formulations of the image captioning problem deviate from the traditional supervised learning paradigm. Novel object captioning aims to describe objects that do not exist in the training data [1, 23, 41, 50, 70]. Feng *et al.* [20] propose unsupervised captioning without using paired image-caption supervision. Kim *et al* [29] focus on learning efficiency and improve the data efficiency by learning from auxiliary unpaired image-caption data.

Self-supervised NLP Models. Self-supervised training of large neural networks on textual data proves to be an important technique in the creation of high-performance NLP models. Several self-supervision signals have been proposed, such as autoregressive language modeling [5, 52], which includes the GPT series of models [6, 58, 59], and masked language modeling, which includes ELMo [56] and BERT-related methods [16, 32, 47].

In this paper, we propose a quick adaptation technique for network weights obtained using the language modeling (LM) objective. However, the proposed technique can easily be applied to other models, as the masked language modeling objective can be converted to the LM objective by masking only the last word in the textual sequence. Unlike neural networks pretrained on multimodal data (e.g., [39, 48, 57, 66, 67, 82, 83]), our method only requires a small amount of multimodal training data and focuses on adapting linguistic knowledge learned from the textual modality.

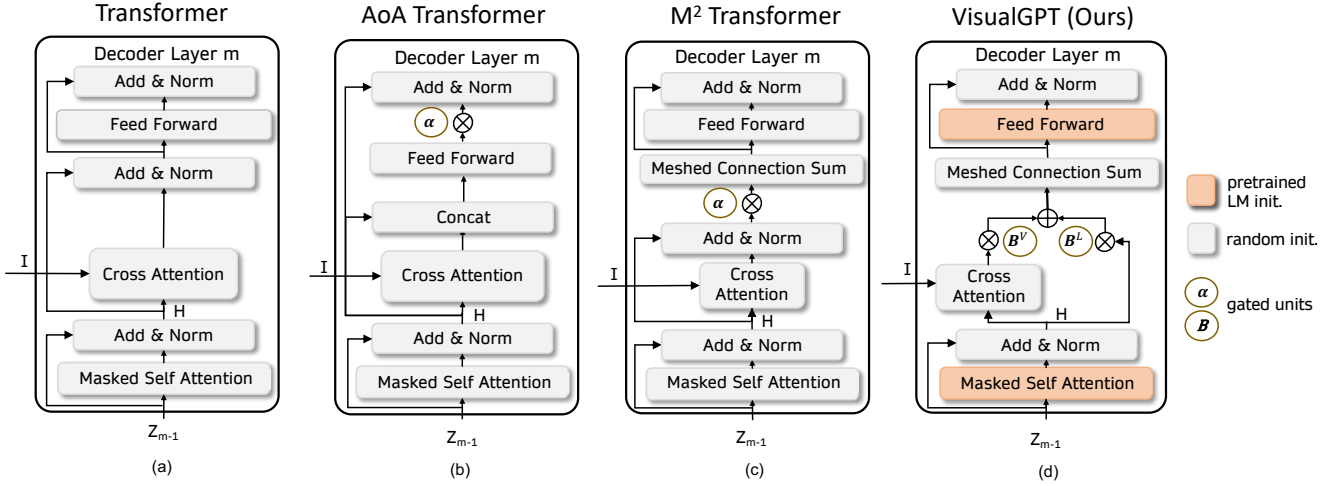


Figure 3. Architectures of vanilla Transformer [68], Transformer with AoA module [24] (AoA Transformer), \mathcal{M}^2 Transformer [13], and VisualGPT. We denote I and H as the visual and language features, respectively. Z_{m-1} is the output from decoder layer $m - 1$. Within the circles, α , B^V and B^L represent different gating units.

3. Preliminaries: Transformer for Captioning

The Transformer [68] has become one of the standard models for image captioning. At its core lies the multi-head dot-product attention mechanism. Taking three input matrices, query Q , key K , and value V , the attention function can be written as

$$\text{Attn}(Q, K, V) = \text{softmax} \left(\frac{(W^q Q)(W^k K)^\top}{\sqrt{D}} \right) W^v V, \quad (1)$$

where W^q , W^k , and W^v are trainable parameters and D is a scaling factor. Intuitively, the attention operation can be seen as encoding $W^q Q$ as convex combination of the row vectors of $W^v V$. The multi-head attention repeats the process with multiple sets of W^q , W^k , and W^v ; the results are concatenated and linearly projected back to the same dimensionality.

In visual captioning tasks, we apply a visual encoder whose output is $I \in \mathbb{R}^{O \times S}$. O is the length of the input sequence, which in this work is a sequence of objects in the image. S is the hidden dimension size. The decoder network outputs words in the caption sequentially.

When decoding word $t+1$, the encoder-decoder attention takes as input the visual encoding I and the current state of the decoder $H \in \mathbb{R}^{t \times S}$. We apply the attention operation with H as the query and I as both the key and the value. The encoder-decoder attention is then

$$\text{EncDecAttn}(H, I) = \text{Attn}(H, I, I). \quad (2)$$

After that, we apply the AddNorm operator, which contains a residual connection and layer normalization [3] and can be written as $\text{LayerNorm}(\text{EncDecAttn}(H, I) + H)$.

Researchers have proposed other variants of the encoder-decoder attention. In Figure 3, we contrast these decoder architectures with the proposed VisualGPT model. The Attention-on-Attention (AoA) module [24] provides an alternative method for combining the visual encoding I and the linguistic information H from the decoder. For another method for combining visual and linguistic information, \mathcal{M}^2 Transformer [13] connects all decoder layers to all encoder layers. In Figure 3, it is represented by the box labeled as *Meshed Connection Sum*.

4. VisualGPT

Pretrained language models (PLMs) such as GPT-2 [59] are trained on data from a single modality. We use a PLM as the caption decoder and feed visual information to the PLM via the encoder-decoder attention, which plays a crucial role in quickly adapting the PLMs.

With the design of the encoder-decoder attention, we aim to carefully balance visual information from the encoder and linguistic knowledge stored in the PLM. During the generation of visual words, such as “person”, “truck”, or “dog”, the model should attend to visual information. In contrast, the generation of determiners or connectives requires only linguistic knowledge. Ideally, we would like to exploit the massive amount of linguistic knowledge stored in the PLM weights (e.g., [44]), while referring to the visual input only when required. To achieve this goal, we introduce a pair of specialized gating units.

4.1. Self-Resurrecting Activation Unit

The encoder-decoder attention $\text{EncDecAttn}(H, I)$ may be seen as encoding the linguistic information H with visual

information I . In VisualGPT, we control the balance between these two modalities using two complementary gates B^{vis} and B^{lan} . The output of this module is

$$B^{\text{vis}} \otimes \text{EncDecAttn}(H, I) + B^{\text{lan}} \otimes H, \quad (3)$$

where \otimes denotes element-wise multiplication. Letting $B^{\text{vis}}[i, j]$ and $B^{\text{lan}}[i, j]$ denote the elements in the matrices, they are computed in pairs as

$$\begin{aligned} B^{\text{vis}}[i, j] &= \sigma(H[i, j]) \mathbb{1}(\sigma(H[i, j]) > \tau), \\ B^{\text{lan}}[i, j] &= (1 - \sigma(H[i, j])) \mathbb{1}(1 - \sigma(H[i, j]) > \tau), \end{aligned} \quad (4)$$

where τ is a predefined threshold hyperparameter and $\mathbb{1}(\cdot)$ is the indicator function, which returns 1 if the inner statement is true and 0 otherwise.

An alternative to SRAU is ordinary complementary gates (OCG), computed as $\sigma(H[i, j])$ and $1 - \sigma(H[i, j])$ (see Figure 4, top left). OCG can output values that are very close to zero. In contrast, with the indicator functions SRAU directly sets values less than the threshold τ to zero, thereby introducing sparsity. When τ is set to 0, SRAU becomes OCG. As the gradient cannot backpropagate through zero gates, SRAU prevents optimization from disrupting pre-trained weights that capture linguistic knowledge. This property is crucial in effective utilizing of pretrained models. In contrast, when the OCG gates output near-zero values, some small but non-zero gradients may still overwrite existing linguistic knowledge.

Another advantage of SRAU is its ability to escape from zero outputs. It is possible for one gate to output zero and have zero gradient while the gradient for the other gate remains usable (e.g., when x in Fig 4 is close to 1.3 or -1.3). The asymmetry allows gradient-based optimization to change the zero-outputting gate by changing the other gate. For this reason, we name these gates self-resurrecting activation units.

The asymmetry of SRAU may appear counter-intuitive. We contrast SRAU with a “normalized” version where the two gates $\tilde{B}^{\text{vis}}[i, j]$ and $\tilde{B}^{\text{lan}}[i, j]$ become symmetric.

$$\begin{aligned} \tilde{B}^{\text{vis}}[i, j] &= \frac{B^{\text{vis}}[i, j]}{B^{\text{vis}}[i, j] + B^{\text{lan}}[i, j]}, \\ \tilde{B}^{\text{lan}}[i, j] &= \frac{B^{\text{lan}}[i, j]}{B^{\text{vis}}[i, j] + B^{\text{lan}}[i, j]}. \end{aligned} \quad (5)$$

These gates lose the asymmetry that enables the self-resurrecting property.

In Figure 4, we visualize OCG, SRAU, and normalized SRAU. In ablation experiments, we show that SRAU outperforms than both OCG and normalized SRAU.

4.2. The Architecture and Training of VisualGPT

For completeness, we introduce the overall architecture for VisualGPT. The image encoder comprising K Transformer layers. Given an image, we extract objects in the

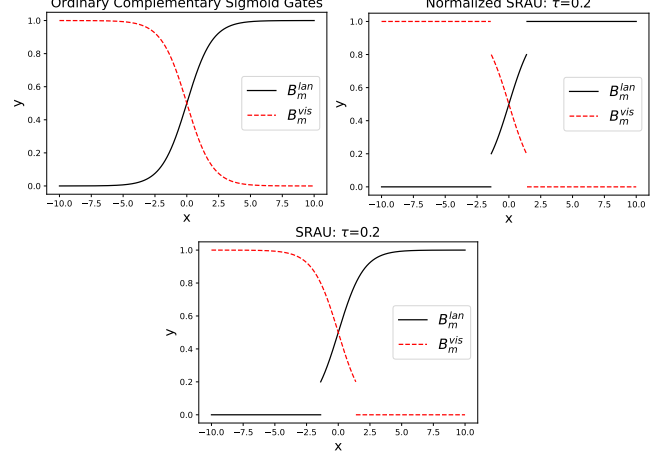


Figure 4. Top Left: Ordinary complementary sigmoid gates. Top Right: Normalized SRAU $\tau=0.2$. Bottom: SRAU $\tau=0.2$. The x-axis indicates the function inputs and the y-axis indicates outputs.

image using an off-the-shelf object detection network. After that, we feed the spatial location into the image encoder. As such, the image encoder outputs I of dimension $S \times O \times K$.

The caption decoder contains M layers and its parameters are initialized from a PLM. We insert the encoder-decoder module, which is randomly initialized. We also apply meshed connections between the encoder and the decoder like in \mathcal{M}^2 Transformer. The network is trained to maximize the probability of the next token w_t conditioned on tokens w_1, \dots, w_{t-1} and the encoder output I . After a predefined number of epochs on supervised learning, we switch to self-critical reinforcement learning [61] with CIDEr as the reward.

5. Experiments

5.1. Datasets and Evaluation Metrics

We evaluate our model on three datasets, MS COCO [43], Conceptual Captions [63], and IU X-ray [15]. MS COCO contains 123,287 images and each of them is annotated with 5 different captions. We follow the Karpathy split [28] for the validation and test set. The Conceptual Captions dataset [63] contains around 3.3M images for training and 28K for validation, with much higher diversity than COCO. As the test data is not publicly available, we instead use the public validation data as our test set, and randomly sample 5000 different image-caption pairs from the training set as the validation set. To create the small training data setup for MS COCO and Conceptual Captions, we randomly sample 0.1%, 0.5% and 1% image-caption pairs as training data, which matches to (567, 2,835 and 5,670 pairs) for COCO and (3,300, 16,500, and 33,000 pairs) for Conceptual Captions. We repeat the experiments 4 times with different random seeds, and report the average performance. We report metrics for BLEU [54], METEOR [4],

Method	PLM	COCO						Conceptual				
		B1	B4	M	R	C	B1	B4	M	R	C	
0.1% training data												
Transformer [68]	None	57.4	13.1	16.7	40.7	40.8	12.4	2.4	4.9	15.2	21.2	
\mathcal{M}^2 Transformer [13]	None	56.9	13.1	16.9	40.6	40.9	13.1	2.8	4.8	15.5	23.5	
AoA Transformer [24]	None	56.6	13.5	15.9	40.7	38.4	11.4	2.4	4.6	14.7	20.9	
X-Transfomer [53]	None	56.7	12.9	16.5	40.6	40.4	12.8	2.7	4.7	15.3	23.1	
OSCAR [39]	BERT	53.8	11.9	17.1	39.5	41.0	12.2	2.4	4.3	14.8	21.9	
Transformer	GPT	56.8	15.3	17.0	41.2	42.9	13.2	2.5	5.0	15.1	21.9	
\mathcal{M}^2 Transformer	GPT	54.9	14.7	16.6	41.1	41.0	11.9	2.6	4.9	15.4	24.0	
AoA Transformer	GPT	55.5	14.4	16.2	40.7	40.1	11.8	2.8	4.6	13.9	20.5	
VisualGPT (Normalized SRAU)	GPT	55.7	15.0	16.8	41.2	42.4	13.3	2.9	5.1	15.8	25.8	
VisualGPT (Our SRAU)	GPT	58.2	16.4	18.5	41.9	45.1	13.9	3.2	5.6	16.7	27.7	
0.5% training data												
Transformer	None	62.8	18.8	19.4	25.2	59.2	13.2	3.3	5.5	16.3	29.6	
\mathcal{M}^2 Transformer	None	63.3	19.4	19.8	45.6	61.3	14.5	3.6	6.0	17.1	32.0	
AoA Transformer	None	63.5	20.2	19.4	45.8	63.9	13.8	3.3	5.6	17.9	31.8	
X-Transformer	None	62.9	19.0	19.6	45.7	62.0	14.2	3.5	5.8	17.3	32.1	
OSCAR	BERT	59.2	18.0	21.0	45.3	60.2	14.4	3.7	6.1	17.2	33.5	
Transformer	GPT	65.1	21.8	20.6	46.6	69.5	16.2	3.8	6.5	18.3	35.6	
\mathcal{M}^2 Transformer	GPT	64.7	21.8	20.7	47.1	68.5	13.9	3.6	6.0	17.2	34.1	
AoA Transformer	GPT	64.2	21.2	20.5	46.5	67.2	14.8	3.6	6.2	17.6	34.1	
VisualGPT (Normalized SRAU)	GPT	65.3	21.8	20.9	47.0	69.3	14.9	3.9	6.1	18.0	35.9	
VisualGPT (Our SRAU)	GPT	66.2	22.1	21.1	47.3	70.3	15.9	4.2	6.7	18.5	37.2	
1% training data												
Transformer	None	66.0	21.9	21.1	47.3	71.9	13.9	3.7	6.3	18.1	37.9	
\mathcal{M}^2 Transformer	None	67.1	23.4	21.3	48.3	73.0	16.0	4.1	6.8	18.9	39.8	
AoA Transformer	None	67.6	23.6	21.5	48.4	75.5	14.9	4.1	6.5	18.6	39.0	
X-Transformer	None	67.0	23.6	21.2	48.1	47.1	15.6	4.0	6.6	18.7	39.5	
OSCAR	BERT	67.2	23.3	22.5	49.1	78.4	16.1	4.2	6.7	18.9	40.6	
Transformer	GPT	68.5	25.1	22.1	49.0	80.5	17.8	4.2	6.7	19.0	40.2	
\mathcal{M}^2 Transformer	GPT	68.2	25.0	22.4	49.2	80.4	15.4	3.9	6.5	17.9	39.1	
AoA Transformer	GPT	68.5	24.6	22.0	48.6	78.4	15.4	3.9	6.5	17.9	38.5	
VisualGPT (Normalized SRAU)	GPT	68.7	25.2	22.3	49.2	80.6	15.3	4.2	6.7	18.3	40.3	
VisualGPT (Our SRAU)	GPT	69.5	25.6	22.6	49.6	80.9	16.3	4.3	6.9	19.3	40.9	

Table 1. Performance of the compared methods training on 0.1%, 0.5% and 1% of MS COCO and Conceptual Caption image-caption pairs. The best performance in each configuration is in bold. Ablated models are marked in gray.

ROUGE [42], and CIDEr [69].

IU X-ray [15] is a radiography dataset containing 7,470 chest X-ray images and 3,955 human-written reports. As the dataset is already small, we follow the original split, which has a training set of 5,226 images and 2,770 reports. Most reports have two images corresponding to the frontal and lateral viewpoints.

5.2. Experimental Settings

Baselines. We compare our model with several state-of-the-art transformer-based models, including:

- Plain Transformer [68].

- AoA Transformer, which inserts an attention-on-attention (AoA) module [24] into every transformer layer, as depicted by Figure 3 (b). Following [13], we slightly update the original AoA network in [24] by replacing the LSTM with Transformers in order to create a fair Transformer-to-Transformer comparison.
- \mathcal{M}^2 Transformer [13], which proposes a meshed connection between encoder and decoder and is one of the best-performing models on MS COCO.
- X-Transformer [53], which employs bilinear pooling to selectively capitalize on visual information and is

Models	B-1	B-2	B-3	B-4	R	M	C
Att2in	22.4	12.9	8.9	6.8	30.8	-	29.7
CoAtt	45.5	28.8	20.5	15.4	36.9	-	27.7
HRGR	43.8	29.8	20.8	15.1	32.2	-	34.3
CMAS-RL	46.4	30.1	21.0	15.4	37.1	-	27.5
Chen <i>et al.</i>	47.0	30.4	21.9	16.5	37.1	18.7	-
VisualGPT (ours)	48.0	31.3	22.2	15.9	37.4	20.5	49.7

Table 2. Performance on the IU X-ray dataset.

one of best-performing models on MS COCO.

- OSCAR [39], which finetunes BERT initialization on image-language dataset.

Since VisualGPT has GPT as the pretrained decoder, for fair comparisons, we also create variants of Transformer, AoA Transformer and \mathcal{M}^2 Transformer with GPT as the decoder. For VisualGPT, we set τ to 0.2 in *all* experiments. We also explored the effect of different τ and find τ in the range of $[0, 0.2]$ to offer the right level of sparsity. For all other baselines, we tune the hyperparameters on the validation set of MS COCO. We train our model and all the baselines in reinforcement learning setting following the work in [13]. Please see the supplemental material for more details on hyperparameters and experimental results.

5.3. Quantitative Results

Small In-domain Training Data. Results on MS COCO and Conceptual Captions are presented in Tables 1. VisualGPT outperforms the best-performing baseline model by 4.1 CIDEr when trained on 0.1% of MS COCO data, 6.4 CIDEr when trained on 0.5% data and 2.5 CIDEr with 1% training data. On Conceptual Caption dataset, VisualGPT also outperforms all the baselines. It outperforms the best baseline model by 4.2 CIDEr under 0.1% training data, 3.5 CIDEr under 0.5% data and 0.3 CIDEr under 1% data.

Comparison with BERT-based model. We compared with OSCAR [39] which is a BERT-based [16] model with good performing results in many benchmarks. We run their model without pretraining on a large-scale image-language corpus for the fair comparison with our model. The main difference between BERT and GPT is their different pre-training objectives, where BERT uses masked language modeling and GPT is the autoregressive prediction of the next word. GPT has more similar learning behaviors to the image captioning model compared to BERT since they are both optimized by autoregressively generating the next language word. The experimental result in Table 1 shows that VisualGPT is better than OSCAR in both datasets, which confirms our selection choice of using GPT as a decoder.

Medical Report Generation. We compared VisualGPT against state-of-the-art medical report generation models

Models	B-1	B-4	M	R	C
Kim <i>et al.</i> [30]	58.1	13.4	15.9	-	36.0
Kim <i>et al.</i> + unpaired	63.0	18.7	20.7	-	55.2
Gu <i>et al.</i> [22]	46.2	5.4	13.2	-	17.7
Feng <i>et al.</i> [20]	58.9	18.6	17.9	-	54.9
VisualGPT (ours)	67.1	24.3	21.9	48.6	75.8

Table 3. Comparison with unsupervised and semi-supervised learning methods using Kim *et al.*’s split of MS COCO. Kim *et al.* employ only 1% images for training in contrast to 1% image-caption pairs from Table 1. Note that Kim *et al.* + unpaired also use the rest of training data as unpaired images and texts. The gray shading denotes baselines that use a large amount of unpaired images and texts during training.

including Att2in [61], CoAtt [26], HRGR [35], CMAS-RL [25] and the model from Chen *et al.* [10]. This dataset only contains around 2,770 medical reports in the training set, which is less than 1% COCO data and poses a data-efficiency challenge. We follow the same experimental setting as in [10]. The results show that VisualGPT outperforms the baselines for most evaluation metrics and creates a new state-of-the-art. It shows the value of leveraging GPT knowledge into the highly specific domain which has very “expensive” and insufficient paired data. We hope our finding could inspire future work in other domains.

Comparison Against Semi-supervised and Unsupervised Methods. Kim *et al.* [30] proposed a semi-supervised learning method to improve the data efficiency of image captioning. They used 1% of images and all their captions as training data, rather than 1% of all the image-caption pairs in Table 1, hence they cover less images since each image is associated to more than 1 caption. For Kim *et al.* + unpaired, they also employ the other 99% of MS COCO as unpaired images and captions for training. We replicate their setup by only training with 1% of images. As shown in Table 3, without using additional unpaired images and captions, the proposed VisualGPT method outperforms Kim *et al.* [30] by 20.6 CIDEr score.

We also compare VisualGPT against unsupervised methods of Gu *et al.* [22] and Feng *et al.* [20], which use tens of millions of unpaired images and captions. Even though these are not fair comparisons, it is encouraging to see VisualGPT surpassing these baselines by utilizing the supervision of only 1133 training images.

5.4. Ablation Studies

Ablation on cross-attention: To fairly compare our SRAU with other cross-attention mechanisms in the baselines, we also initialize their decoder with 12-layer GPT and keep the same encoder as VisualGPT. We contrast between plain cross-attention, meshed cross-attention, and attention-on-

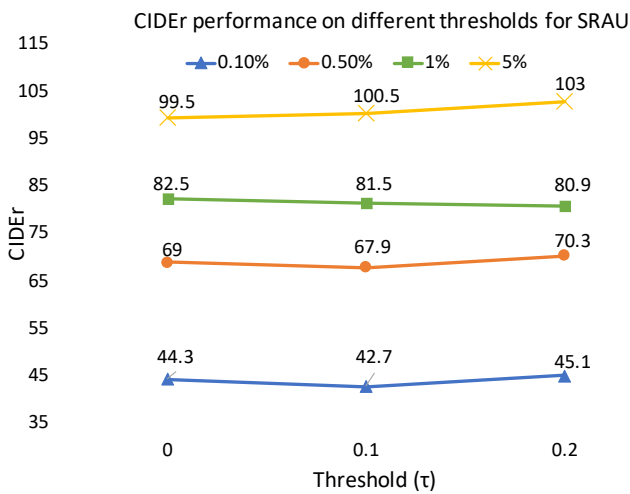


Figure 5. CIDEr performance v.s. different thresholds τ with 0.1% 0.5%, 1% and 5% training data.

attention (AoA) modules. For AoA Transformer, we add the AoA module on top of cross-attention. Table 1 shows the results, which demonstrate that SRAU is better than other cross-attention modules in exploiting the GPT knowledge within the image-caption task.

Ablation on SRAU: We create an ablation called *Normalized SRAU*, where we replace the SRAU with the normalized SRAU (see Figure 4) and use GPT2 initialization. We provided the results in table 1. The normalized SRAU results in substantially lowered performance, decreasing CIDEr from full VisualGPT by 2.7, 1.0, and 0.3 respectively on the three setups on MS COCO, and it also decreases from Full VisualGPT by 2.2, 1.3 and 0.6 respectively on Conceptual Caption. This demonstrates that the self-resurrecting property is beneficial for learning from small data. We experimented with Leaky ReLU and GELU, which ameliorate zero gradients, but the training crashed due to the lack of upper limits for function values.

We explored different τ among (0, 0.1 0.2) and show their CIDEr performance on different percentage of COCO training data in the Figure 5. $\tau=0$ is equivalent to ordinary complementary sigmoid gates. We can observe that $\tau = 0.2$ can give us the best performance in most cases, indicating the usefulness of incorporating sparsity in our SRAU complementary gates.

5.5. Human Study

In addition to automatic evaluation metrics, we conduct two human studies to further evaluate the quality of generated captions. In the first study, we asked participants directly for preference over generated captions. We randomly selected 250 test images from the three setups of

Method	0.1% data	0.5% data	1% data
Transformer	18.4%	17.2%	16.8%
AoA Transformer	11.5%	20.9%	25.0%
\mathcal{M}^2 Transformer	30.9%	22.8%	20.8%
VisualGPT	39.2%	39.1%	37.4%

Table 4. The percentage of votes received by VisualGPT and baseline models under different quantity of training data.

Q1. Does the caption miss things shown in the image?

Answer	Ours	\mathcal{M}^2 Transformer	Transformer	AoA	GT
No	719	624	633	621	973
Yes	367	438	456	447	73
No Rate	0.66	0.59	0.58	0.58	0.93

Q2. Does the caption describe things not in the image?

Answer	Ours	\mathcal{M}^2 Transformer	Transformer	AoA	GT
No	720	692	633	655	448
Yes	360	418	423	412	43
No Rate	0.67	0.62	0.60	0.61	0.96

Table 5. Human evaluation of object hallucination and omission. GT denotes the ground-truth captions.

	GT: the lady is sitting on the wood bench
Ours	a woman sitting on a bench in a park
attention	0.7 0.78 0.82 0.76 0.8 0.96 0.8 0.69 0.85
	GT: a laptop with a keyboard and mouse are on this desk
Ours	a laptop sitting on a desk with a mouse
attention	0.7 0.78 0.81 0.7 0.7 0.92 0.85 0.64 0.76
	GT: a cat is sitting in front of a television
Ours	a cat is sitting in front of a television
attention	0.8 0.86 0.8 0.83 0.7 0.72 0.6 0.71 0.93
	GT: a number of people sitting on a snowy surface with skis
Ours	a couple of people sitting on a snowy surface
attention	0.8 0.87 0.71 0.85 0.91 0.76 0.71 0.94 0.95

Figure 6. Visual scores of words in generated captions. We show the raw visual scores and highlight them according to normalized visual scores. High visual scores are in blue and low scores in red.

0.1%, 0.5%, and 1% training data. For every image, we generated one caption from VisualGPT and each of three high-performing baselines from Table 1, Transformer [68], \mathcal{M}^2 Transformer [13], and AoA Transformer [24], all with three decoder layers. Every image was evaluated by 5 different Turkers, who chose the caption that most accurately described the image content. We received 3750 (250 images

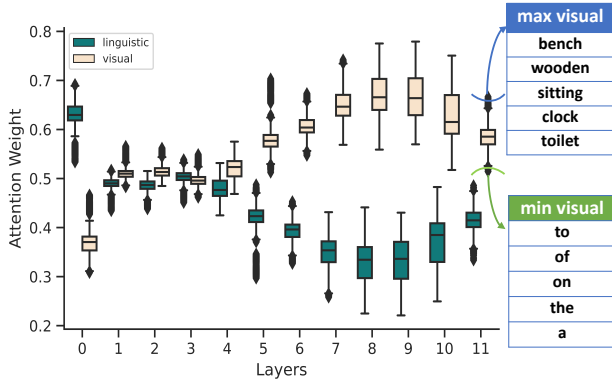


Figure 7. Distributions of linguistic attention (B^{lan}) and visual attention (B^{vis}) at every decoding layer. We also show the words generated with the highest and lowest visual attention.

$\times 5$ Turkers $\times 3$ setups) valid responses.

We summarize the results in Table 4. Overall, the captions generated by VisualGPT received the largest share of votes, 39.2% for the 0.1% training data split, 39.1% for the 0.5% split, and 37.4% for the 1% split. For each training setup, we conducted Pearson’s Chi-square test [55], which shows the differences are statistical significant with $p < 0.05$ in all cases.

In the second study, we evaluate if using pretrained language models introduces excessive linguistic prior that could cause the known object hallucination problem [62]. From the models trained using 1% COCO data. We randomly sampled 250 images with the generated caption from each model. For each image, we asked 5 different participants if the caption (1) described non-existent objects or (2) missed objects existing in the image. To catch random clickers, we created 5 images with verified captions, so that we knew the right answers of these questions. Participants who answered these questions wrongly were considered unreliable and removed from the results.

The results are in Table 5. Compared to the baselines, VisualGPT has less hallucination and higher coverage of objects. The study also finds that the ground-truth captions has the least amount of hallucination and highest coverage of objects in the image. This finding lends positive support to the validity of the experimental protocol.

5.6. Analysis

In this section, we visually examine examples from the VisualGPT model trained on 1% of MS COCO. First, we show example captions generated by VisualGPT in Figure 6 and the associated B^{vis} at the last decoder layer. Note that for every word generated, we have a 768-dimensional visual gate vector, which is a slice of B^{vis} at different decoding time steps. We take the mean of the gate vector as the visual score for that word. After that, we normalize

the visual scores across the dataset to the $[0, 1]$ interval and highlight the words accordingly. Blue indicates high visual scores and red indicates low visual scores. We observe that, in agreement with our intuition, VisualGPT assigns high visual scores to words like “desk” and “snowy surface” and low visual scores to determiners and prepositions.

In Figure 7, we plot the distribution of B^{vis} and B^{lan} at every decoder layer as a box-and-whisker diagram. We also show the words with the highest and lowest visual scores, which are again in line with our expectations. Additionally, we observe that, going from layer 0 to layer 9, the decoder makes increasing use of visual information, but the uppermost layers, 10 and 11, make more balanced use of information. We hypothesize that the low layers focus on low-level linguistics like syntax, whereas the middle layers learn to fuse linguistic information with visual information. Finally, the two information sources become balanced in the uppermost layers.

5.7. Limitation

One limitation of our proposal is that, as experiments in the supplementary material show, the gap between baseline models and VisualGPT gradually vanishes as in-domain training data increase. The phenomenon is more pronounced in COCO than Conceptual Captions, which has a more diverse vocabulary. We hypothesize that linguistic knowledge from pretrained models is the most useful when the training data are small and do not provide sufficient coverage of the vocabulary.

6. Conclusions

We present VisualGPT, a data efficient image captioning model which leverages the linguistic knowledge from the pretrained language model. To bridge the semantic gap between different modalities, we design a novel encoder-decoder attention mechanism with an unsaturated rectified gating function. We evaluate our model on 0.1%, 0.5% and 1.0% of MS COCO and Conceptual Captions, and IU X-ray, a small medical imaging report dataset. VisualGPT achieves the state-of-the-art result on IU X-ray and outperforms strong baseline models.

VisualGPT may solve the realistic need when training captioning models on low-resource languages or highly specialized domains, where it could be challenging to find annotators to collect a large amount of data.

Acknowledgments. This work is funded by KAUST BAS/1/1685-01-0, KAUST-FCC/1/2533-17-01, and National Research Foundation Fellowship (NRF-NRFF13-2021-0006), Singapore.

References

- [1] Harsh Agrawal, Karan Desai, Yufei Wang, Xinlei Chen, Rishabh Jain, Mark Johnson, Dhruv Batra, Devi Parikh, Stefan Lee, and Peter Anderson. nocaps: novel object captioning at scale. In *ICCV*, 2019. [1](#), [2](#)
- [2] Peter Anderson, Xiaodong He, Chris Buehler, Damien Teney, Mark Johnson, Stephen Gould, and Lei Zhang. Bottom-up and top-down attention for image captioning and visual question answering. In *CVPR*, 2018. [2](#)
- [3] Jimmy Lei Ba, Jamie Ryan Kiros, and Geoffrey E. Hinton. Layer normalization. *arXiv 1607.06450*, 2016. [3](#)
- [4] Satanjeev Banerjee and Alon Lavie. Meteor: An automatic metric for mt evaluation with improved correlation with human judgments. In *Proceedings of the acl workshop on intrinsic and extrinsic evaluation measures for machine translation and/or summarization*, 2005. [4](#)
- [5] Yoshua Bengio, Réjean Ducharme, Pascal Vincent, and Christian Jauvin. A neural probabilistic language model. *Journal of machine learning research*, 3(Feb), 2003. [2](#)
- [6] Tom B Brown, Benjamin Mann, Nick Ryder, Melanie Subbiah, Jared Kaplan, Prafulla Dhariwal, Arvind Neelakantan, Pranav Shyam, Girish Sastry, Amanda Askell, et al. Language models are few-shot learners. *arXiv preprint arXiv:2005.14165*, 2020. [1](#), [2](#)
- [7] Paweł Budzianowski and Ivan Vulic. Hello, it's GPT-2 - how can I help you? towards the use of pretrained language models for task-oriented dialogue systems. In Alexandra Birch, Andrew M. Finch, Hiroaki Hayashi, Ioannis Konstas, Thang Luong, Graham Neubig, Yusuke Oda, and Katsuhiro Sudoh, editors, *EMNLP-IJCNLP*. Association for Computational Linguistics, 2019. [1](#)
- [8] Long Chen, Hanwang Zhang, Jun Xiao, Liqiang Nie, Jian Shao, Wei Liu, and Tat-Seng Chua. Sca-cnn: Spatial and channel-wise attention in convolutional networks for image captioning. In *CVPR*, 2017. [2](#)
- [9] Shizhe Chen, Qin Jin, Peng Wang, and Qi Wu. Say as you wish: Fine-grained control of image caption generation with abstract scene graphs. In *CVPR*, 2020. [2](#)
- [10] Zhihong Chen, Yan Song, Tsung-Hui Chang, and Xiang Wan. Generating radiology reports via memory-driven transformer. In *EMNLP*, 2020. [6](#)
- [11] Cesc Chunseong Park, Byeongchang Kim, and Gunhee Kim. Attend to you: Personalized image captioning with context sequence memory networks. In *CVPR*, 2017. [2](#)
- [12] Marcella Cornia, Lorenzo Baraldi, and Rita Cucchiara. Show, control and tell: A framework for generating controllable and grounded captions. In *CVPR*, 2019. [2](#)
- [13] Marcella Cornia, Matteo Stefanini, Lorenzo Baraldi, and Rita Cucchiara. Meshed-memory transformer for image captioning. In *CVPR*, 2020. [1](#), [2](#), [3](#), [5](#), [6](#), [7](#)
- [14] Bo Dai, Sanja Fidler, Raquel Urtasun, and Dahua Lin. Towards diverse and natural image descriptions via a conditional gan. In *ICCV*, 2017. [2](#)
- [15] Dina Demner-Fushman, Marc D Kohli, Marc B Rosenman, Sonya E Shooshan, Laritza Rodriguez, Sameer Antani, George R Thoma, and Clement J McDonald. Preparing a collection of radiology examinations for distribution and retrieval. *Journal of the American Medical Informatics Association*, 23(2), 2016. [1](#), [2](#), [4](#), [5](#)
- [16] Jacob Devlin, Ming-Wei Chang, Kenton Lee, and Kristina Toutanova. Bert: Pre-training of deep bidirectional transformers for language understanding. In *NAACL*, 2019. [1](#), [2](#), [6](#)
- [17] Li Dong, Nan Yang, Wenhui Wang, Furu Wei, Xiaodong Liu, Yu Wang, Jianfeng Gao, Ming Zhou, and Hsiao-Wuen Hon. Unified language model pre-training for natural language understanding and generation. In *NeurIPS*, 2019. [1](#)
- [18] Obeida ElJundi., Mohamad Dhaybi., Kotaiba Mokadam., Hazem Hajj., and Daniel Asmar. Resources and end-to-end neural network models for arabic image captioning. In *Proceedings of the 15th International Joint Conference on Computer Vision, Imaging and Computer Graphics Theory and Applications - Volume 5: VISAPP*, pages 233–241. IN-STICC, SciTePress, 2020. [1](#)
- [19] Ali Farhadi, Mohsen Hejrati, Mohammad Amin Sadeghi, Peter Young, Cyrus Rashtchian, Julia Hockenmaier, and David Forsyth. Every picture tells a story: Generating sentences from images. In *ECCV*. Springer, 2010. [2](#)
- [20] Yang Feng, Lin Ma, Wei Liu, and Jiebo Luo. Unsupervised image captioning. In *CVPR*, 2019. [2](#), [6](#)
- [21] Sergey Golovanov, Rauf Kurbanov, Sergey Nikolenko, Kyryl Truskovskyi, Alexander Tselousov, and Thomas Wolf. Large-scale transfer learning for natural language generation. In *ACL*, 2019. [1](#)
- [22] Jiuxiang Gu, Shafiq Joty, Jianfei Cai, and Gang Wang. Unpaired image captioning by language pivoting. In *ECCV*, 2018. [6](#)
- [23] Lisa Anne Hendricks, Subhashini Venugopalan, Marcus Rohrbach, Raymond Mooney, Kate Saenko, and Trevor Darrell. Deep compositional captioning: Describing novel object categories without paired training data. In *CVPR*, 2016. [1](#), [2](#)
- [24] Lun Huang, Wenmin Wang, Jie Chen, and Xiao-Yong Wei. Attention on attention for image captioning. In *ICCV*, 2019. [1](#), [2](#), [3](#), [5](#), [7](#)
- [25] Baoyu Jing, Zeya Wang, and Eric Xing. Show, describe and conclude: On exploiting the structure information of chest x-ray reports. In *ACL*, 2019. [6](#)
- [26] Baoyu Jing, Pengtao Xie, and Eric Xing. On the automatic generation of medical imaging reports. In *ACL*, 2018. [6](#)
- [27] Justin Johnson, Andrej Karpathy, and Li Fei-Fei. Densecap: Fully convolutional localization networks for dense captioning. In *CVPR*, 2016. [2](#)
- [28] Andrej Karpathy and Li Fei-Fei. Deep visual-semantic alignments for generating image descriptions. In *CVPR*, 2015. [1](#), [4](#)
- [29] Dong-Jin Kim, Jinsoo Choi, Tae-Hyun Oh, and In So Kweon. Image captioning with very scarce supervised data: Adversarial semi-supervised learning approach. In Kentaro Inui, Jing Jiang, Vincent Ng, and Xiaojun Wan, editors, *EMNLP-IJCNLP*. Association for Computational Linguistics, 2019. [2](#)

- [30] Dong-Jin Kim, Jinsoo Choi, Tae-Hyun Oh, and In So Kweon. Image captioning with very scarce supervised data: Adversarial semi-supervised learning approach. In *EMNLP*, Hong Kong, China, Nov. 2019. Association for Computational Linguistics. 6
- [31] Girish Kulkarni, Visruth Premraj, Vicente Ordonez, Sagnik Dhar, Siming Li, Yejin Choi, Alexander C Berg, and Tamara L Berg. Babytalk: Understanding and generating simple image descriptions. *TPAMI*, 35(12), 2013. 1, 2
- [32] Zhenzhong Lan, Mingda Chen, Sebastian Goodman, Kevin Gimpel, Piyush Sharma, and Radu Soricut. Albert: A lite bert for self-supervised learning of language representations. In *ICLR*, 2019. 2
- [33] Kuang-Huei Lee, Xi Chen, Gang Hua, Houdong Hu, and Xiaodong He. Stacked cross attention for image-text matching. In *ECCV*, 2018. 2
- [34] Mike Lewis, Yinhan Liu, Naman Goyal, Marjan Ghazvininejad, Abdelrahman Mohamed, Omer Levy, Veselin Stoyanov, and Luke Zettlemoyer. BART: Denoising sequence-to-sequence pre-training for natural language generation, translation, and comprehension. 2019. 1
- [35] Christy Y Li, Xiaodan Liang, Zhiting Hu, and Eric P Xing. Hybrid retrieval-generation reinforced agent for medical image report generation. In *NeurIPS*, 2018. 6
- [36] Guang Li, Linchao Zhu, Ping Liu, and Yi Yang. Entangled transformer for image captioning. In *ICCV*, 2019. 2
- [37] Siming Li, Girish Kulkarni, Tamara Berg, Alexander Berg, and Yejin Choi. Composing simple image descriptions using web-scale n-grams. In *CoNLL*, 2011. 2
- [38] Xiangyang Li and Shuqiang Jiang. Know more say less: Image captioning based on scene graphs. *IEEE Transactions on Multimedia*, 21(8), 2019. 2
- [39] Xiuju Li, Xi Yin, Chunyuan Li, Pengchuan Zhang, Xiaowei Hu, Lei Zhang, Lijuan Wang, Houdong Hu, Li Dong, Furu Wei, et al. Oscar: Object-semantics aligned pre-training for vision-language tasks. In *ECCV*. Springer, 2020. 2, 5, 6
- [40] Yuan Li, Xiaodan Liang, Zhiting Hu, and Eric P Xing. Hybrid retrieval-generation reinforced agent for medical image report generation. In *NeurIPS*. 2018. 1
- [41] Yehao Li, Ting Yao, Yingwei Pan, Hongyang Chao, and Tao Mei. Pointing novel objects in image captioning. In *CVPR*, 2019. 2
- [42] Chin-Yew Lin and Eduard Hovy. Manual and automatic evaluation of summaries. In *Proceedings of the ACL-02 Workshop on Automatic Summarization-Volume 4*, 2002. 5
- [43] Tsung-Yi Lin, Michael Maire, Serge Belongie, James Hays, Pietro Perona, Deva Ramanan, Piotr Dollár, and C Lawrence Zitnick. Microsoft COCO: Common objects in context. In *ECCV*. Springer, 2014. 1, 4
- [44] Nelson F Liu, Matt Gardner, Yonatan Belinkov, Matthew E Peters, and Noah A Smith. Linguistic knowledge and transferability of contextual representations. In *NAACL*, 2019. 3
- [45] Siqi Liu, Zhenhai Zhu, Ning Ye, Sergio Guadarrama, and Kevin Murphy. Improved image captioning via policy gradient optimization of SPIDER. In *ICCV*, 2017. 2
- [46] Yinhan Liu, Myle Ott, Naman Goyal, Jingfei Du, Mandar Joshi, Danqi Chen, Omer Levy, Mike Lewis, Luke Zettlemoyer, and Veselin Stoyanov. RoBERTa: A robustly optimized BERT pretraining approach. *arXiv Preprint*, arXiv 1907.11692, 2019. 1
- [47] Yinhan Liu, Myle Ott, Naman Goyal, Jingfei Du, Mandar Joshi, Danqi Chen, Omer Levy, Mike Lewis, Luke Zettlemoyer, and Veselin Stoyanov. Roberta: A robustly optimized bert pretraining approach. 2019. 2
- [48] Jiasen Lu, Dhruv Batra, Devi Parikh, and Stefan Lee. Vilbert: Pretraining task-agnostic visiolinguistic representations for vision-and-language tasks. In Hanna M. Wallach, Hugo Larochelle, Alina Beygelzimer, Florence d’Alché-Buc, Emily B. Fox, and Roman Garnett, editors, *NeurIPS*, 2019. 2
- [49] Jiasen Lu, Caiming Xiong, Devi Parikh, and Richard Socher. Knowing when to look: Adaptive attention via a visual sentinel for image captioning. In *CVPR*, 2017. 2
- [50] Jiasen Lu, Jianwei Yang, Dhruv Batra, and Devi Parikh. Neural baby talk. In *CVPR*, 2018. 2
- [51] Stephen Merity, Caiming Xiong, James Bradbury, and Richard Socher. Pointer sentinel mixture models. 2017. 2
- [52] Tomáš Mikolov, Stefan Kombrink, Lukáš Burget, Jan Černocký, and Sanjeev Khudanpur. Extensions of recurrent neural network language model. In *ICASSP*. IEEE, 2011. 2
- [53] Yingwei Pan, Ting Yao, Yehao Li, and Tao Mei. X-linear attention networks for image captioning. In *Proceedings of the IEEE/CVF Conference on Computer Vision and Pattern Recognition*, pages 10971–10980, 2020. 5
- [54] Kishore Papineni, Salim Roukos, Todd Ward, and Wei-Jing Zhu. Bleu: a method for automatic evaluation of machine translation. In *ACL*, 2002. 4
- [55] Karl Pearson. X. on the criterion that a given system of deviations from the probable in the case of a correlated system of variables is such that it can be reasonably supposed to have arisen from random sampling. *The London, Edinburgh, and Dublin Philosophical Magazine and Journal of Science*, 50(302), 1900. 8
- [56] Matthew E Peters, Mark Neumann, Mohit Iyyer, Matt Gardner, Christopher Clark, Kenton Lee, and Luke Zettlemoyer. Deep contextualized word representations. In *NAACL-HLT*, 2018. 2
- [57] Di Qi, Lin Su, Jia Song, Edward Cui, Taroon Bharti, and Arun Sacheti. Imagebert: Cross-modal pre-training with large-scale weak-supervised image-text data. *arXiv preprint arXiv:2001.07966*, 2020. 2
- [58] Alec Radford, Karthik Narasimhan, Tim Salimans, and Ilya Sutskever. Improving language understanding by generative pre-training. 2018. 1, 2
- [59] Alec Radford, Jeffrey Wu, Rewon Child, David Luan, Dario Amodei, and Ilya Sutskever. Language models are unsupervised multitask learners. *OpenAI blog*, 1(8), 2019. 1, 2, 3
- [60] Colin Raffel, Noam Shazeer, Adam Roberts, Katherine Lee, Sharan Narang, Michael Matena, Yanqi Zhou, Wei Li, and Peter J. Liu. Exploring the limits of transfer learning with a unified text-to-text transformer. *Journal of Machine Learning Research*, 21:1–67, 2020. 1
- [61] Steven J Rennie, Etienne Marcheret, Youssef Mroueh, Jerret Ross, and Vaibhava Goel. Self-critical sequence training for image captioning. In *CVPR*, 2017. 2, 4, 6

- [62] Anna Rohrbach, Lisa Anne Hendricks, Kaylee Burns, Trevor Darrell, and Kate Saenko. Object hallucination in image captioning. In *EMNLP*, 2018. 8
- [63] Piyush Sharma, Nan Ding, Sebastian Goodman, and Radu Soricut. Conceptual captions: A cleaned, hypernymed, image alt-text dataset for automatic image captioning. In *ACL*, 2018. 1, 4
- [64] Rakshith Shetty, Marcus Rohrbach, Lisa Anne Hendricks, Mario Fritz, and Bernt Schiele. Speaking the same language: Matching machine to human captions by adversarial training. In *ICCV*, 2017. 2
- [65] Richard Socher and Li Fei-Fei. Connecting modalities: Semi-supervised segmentation and annotation of images using unaligned text corpora. In *CVPR*. IEEE, 2010. 2
- [66] Weijie Su, Xizhou Zhu, Yue Cao, Bin Li, Lewei Lu, Furu Wei, and Jifeng Dai. ViL-bert: Pre-training of generic visual-linguistic representations. In *ICLR*, 2020. 2
- [67] Hao Tan and Mohit Bansal. LXMERT: learning cross-modality encoder representations from transformers. In Kentaro Inui, Jing Jiang, Vincent Ng, and Xiaojun Wan, editors, *EMNLP-IJCNLP*. ACL, 2019. 2
- [68] Ashish Vaswani, Noam Shazeer, Niki Parmar, Jakob Uszkoreit, Llion Jones, Aidan N Gomez, Łukasz Kaiser, and Illia Polosukhin. Attention is all you need. In *NeurIPS*, 2017. 3, 5, 7
- [69] Ramakrishna Vedantam, C Lawrence Zitnick, and Devi Parikh. Cider: Consensus-based image description evaluation. In *CVPR*, 2015. 5
- [70] Subhashini Venugopalan, Lisa Anne Hendricks, Marcus Rohrbach, Raymond Mooney, Trevor Darrell, and Kate Saenko. Captioning images with diverse objects. In *CVPR*, 2017. 2
- [71] Oriol Vinyals, Alexander Toshev, Samy Bengio, and Dumitru Erhan. Show and tell: Lessons learned from the 2015 MSCOCO image captioning challenge. *TPAMI*, 39(4), 2016. 2
- [72] Qingzhong Wang and Antoni B. Chan. Cnn+cnn: Convolutional decoders for image captioning. *arXiv 1805.09019*, 2018. 2
- [73] Yufei Wang, Zhe Lin, Xiaohui Shen, Scott Cohen, and Garrison W Cottrell. Skeleton key: Image captioning by skeleton-attribute decomposition. In *CVPR*, 2017. 2
- [74] Yike Wu, Shiwan Zhao, Jia Chen, Ying Zhang, Xiaojie Yuan, and Zhong Su. Improving captioning for low-resource languages by cycle consistency. In *2019 IEEE International Conference on Multimedia and Expo (ICME)*, pages 362–367, 2019. 1
- [75] Kelvin Xu, Jimmy Ba, Ryan Kiros, Kyunghyun Cho, Aaron Courville, Ruslan Salakhudinov, Rich Zemel, and Yoshua Bengio. Show, attend and tell: Neural image caption generation with visual attention. In *ICML*, 2015. 1, 2
- [76] Xu Yang, Kaihua Tang, Hanwang Zhang, and Jianfei Cai. Auto-encoding scene graphs for image captioning. In *CVPR*, 2019. 2
- [77] Zhilin Yang, Zihang Dai, Yiming Yang, Jaime Carbonell, Russ R Salakhutdinov, and Quoc V Le. Xlnet: Generalized autoregressive pretraining for language understanding. In *NeurIPS*, 2019. 1
- [78] Zhilin Yang, Ye Yuan, Yuexin Wu, William W Cohen, and Russ R Salakhutdinov. Review networks for caption generation. In D. Lee, M. Sugiyama, U. Luxburg, I. Guyon, and R. Garnett, editors, *NeurIPS*, volume 29, 2016. 2
- [79] Benjamin Z Yao, Xiong Yang, Liang Lin, Mun Wai Lee, and Song-Chun Zhu. I2t: Image parsing to text description. *Proceedings of the IEEE*, 98(8), 2010. 2
- [80] Ting Yao, Yingwei Pan, Yehao Li, and Tao Mei. Exploring visual relationship for image captioning. In *ECCV*, 2018. 2
- [81] Ting Yao, Yingwei Pan, Yehao Li, and Tao Mei. Hierarchy parsing for image captioning. In *ICCV*, 2019. 2
- [82] Pengchuan Zhang, Xiujun Li, Xiaowei Hu, Jianwei Yang, Lei Zhang, Lijuan Wang, Yejin Choi, and Jianfeng Gao. Vinvl: Revisiting visual representations in vision-language models. In *Proceedings of the IEEE/CVF Conference on Computer Vision and Pattern Recognition*, pages 5579–5588, 2021. 2
- [83] Mingchen Zhuge, Dehong Gao, Deng-Ping Fan, Linbo Jin, Ben Chen, Haoming Zhou, Minghui Qiu, and Ling Shao. Kaleido-bert: Vision-language pre-training on fashion domain. In *Proceedings of the IEEE/CVF Conference on Computer Vision and Pattern Recognition*, pages 12647–12657, 2021. 2